

## Microstructural features of $\text{Mg}_x\text{C}_y\text{Ni}_3$ superconducting materials

J. Q. Li,<sup>1,2</sup> L. J. Wu,<sup>1</sup> L. Li,<sup>2</sup> and Y. Zhu<sup>1</sup>

<sup>1</sup>Material Science Division, Brookhaven National Laboratory, Upton, New York 11973

<sup>2</sup>Institute of Physics, Chinese Academy of Sciences, Beijing 100080, People's Republic of China

(Received 17 September 2001; published 11 January 2002)

Structural investigations on a series of superconducting materials with nominal compositions of  $\text{Mg}_x\text{C}_y\text{Ni}_3$  ( $1.0 < x < 1.3, 1.0 < y < 1.55$ ) have revealed evident structural inhomogeneity. Regular domains, with an average size as small as  $\sim 4$  nm, appear commonly in the superconducting materials with  $T_c > 6$  K. This structural phenomenon can be qualitatively explained in terms of the perovskite cubic structure  $\text{MgCNi}_3$  modulated locally by the variable stoichiometry on the C sites. The presence of the local C deficiency could be a dominant factor affecting the crystal structure and superconductivity.

DOI: 10.1103/PhysRevB.65.052506

PACS number(s): 74.62.Bf, 61.14.Lj, 68.37.Lp

Recently, superconductivity has been discovered in the intermetallic compounds  $\text{MgB}_2$  at 39 K (Ref. 1) and  $\text{MgCNi}_3$  at  $\sim 8$  K.<sup>2</sup> The metallic  $\text{MgCNi}_3$  compound has a simple cubic perovskite structure, and becomes superconducting without any doping at low temperature. Recent theoretical and experimental investigations demonstrated that the electronic states at the Fermi surface of  $\text{MgCNi}_3$  are dominated by the  $3d$  orbitals of Ni.<sup>3</sup> Since elemental Ni is a ferromagnetic metal, a high proportion of Ni in this compound suggests that magnetic interactions may play an important role to understand the low-temperature properties of this superconductor. Previously, a variety of compounds with nominal compositions of  $\text{MgCNi}_3$  for  $0.5 < x < 1.25$  has been reported, and all materials were assigned to the perovskite structure type by analogy.<sup>4,5</sup> Recent structural and superconductivity analyses demonstrated that the suitable excesses of Mg and C in the initial materials are favorable to the formation of superconducting phase,<sup>2,6</sup> and the optimum composition of starting materials is proposed to be  $\text{Mg}_{1.2}\text{C}_{1.45}\text{Ni}_3$ .<sup>6</sup> In present study, the microstructural properties of  $\text{Mg}_x\text{C}_y\text{Ni}_3$  ( $1.0 < x < 1.3, 1.0 < y < 1.55$ ) have been discussed. Especially, the structural inhomogeneity in superconducting samples has been extensively analyzed by means of transmission electron microscopy (TEM).

In our study, alloy samples of  $\text{Mg}_x\text{C}_y\text{Ni}_3$  ( $1.0 < x < 1.3, 0.7 < y < 1.55$ ) were prepared by the conventional method as reported in Ref. 2. The measurements of physical properties indicated that the superconducting  $T_c$  of  $\text{Mg}_x\text{C}_y\text{Ni}_3$  materials is sensitive to the C content.<sup>6</sup> The highest  $T_c$  ( $\sim 7$  K) is obtained in the material with nominal composition  $\text{Mg}_{1.2}\text{C}_{1.4}\text{Ni}_3$ . The results of x-ray diffraction suggested that the main phase in all samples has the cubic structure with lattice parameter  $a = 0.383$  nm (space group  $Pm\bar{3}m$ ).<sup>2</sup> Specimens for TEM observations were polished mechanically to a thickness of around  $50 \mu\text{m}$ , dipped to  $20 \mu\text{m}$ , and then ion milled for 3 h. The TEM investigations were performed on JEOL 3000F electron microscope operating at the voltage of 300 kV.

TEM observations indicated that all samples with the nominal compositions of  $\text{Mg}_x\text{C}_y\text{Ni}_3$  ( $1.1 < x < 1.2, 1.2 < y < 1.50$ ) have apparently inhomogeneous microstructure, complex domains with an average size varying from 1 to 10

nm appear commonly. For better understanding the microstructure properties of the superconducting phase, we will focus our attention on the sample with nominal composition of  $\text{Mg}_{1.2}\text{C}_{1.4}\text{Ni}_3$ , which shows a sharp superconducting transition at around 7 K, as illustrated in Fig. 1. Some data from other samples will be partially cited for facilitating the comparisons and discussions. For instance, we display the temperature dependence of resistivity (upper panel) and magnetization (lower panel) for  $\text{Mg}_{1.2}\text{C}_{1.4}\text{Ni}_3$  and  $\text{Mg}_{1.1}\text{C}_{1.2}\text{Ni}_3$  in Fig. 1, illustrating the evident effect of nominal composition on the superconductivity;  $\text{Mg}_{1.1}\text{C}_{1.2}\text{Ni}_3$  exhibits a broadened superconducting transition at lower temperature.

TEM observations along the relevant directions have revealed that the superconducting phase in the material with nominal composition of  $\text{Mg}_{1.2}\text{C}_{1.4}\text{Ni}_3$  has a cubic average structure,<sup>2</sup> and, in general, shows up complex domain structure. In order to primarily characterize the essential structural properties of the superconducting phase, we have chosen several thin areas with relatively large domain size ( $\sim 10$  nm), and, expected to obtain the homogenous structure corresponding to the  $\text{MgCNi}_3$  crystal within one domain. Figs. 1(a) and (b) show selected-area electron diffraction (SAED)

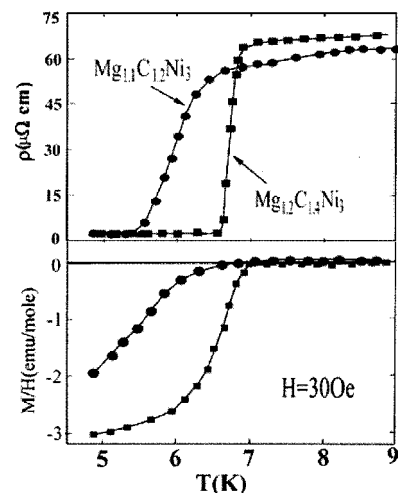


FIG. 1. Temperature dependence of resistivity (upper panel) and magnetization (lower panel) for  $\text{Mg}_{1.1}\text{C}_{1.2}\text{Ni}_3$  and  $\text{Mg}_{1.2}\text{C}_{1.4}\text{Ni}_3$  with a sharp transition at  $\sim 7$  K.

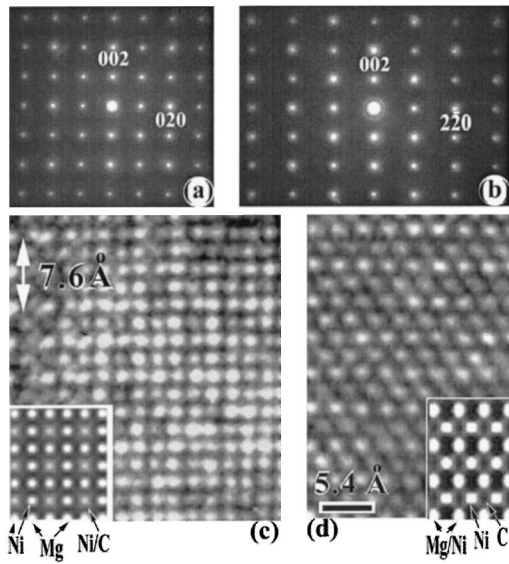


FIG. 2. (a), (b) Electron diffraction patterns of  $\text{MgCNi}_3$  taken along the  $[100]$  and  $[110]$  zone-axis directions, respectively. (c), (d) High-resolution images showing the atomic structure projected along the  $\langle 100 \rangle$  and  $\langle 110 \rangle$  directions.

patterns along the  $[100]$ - and  $[110]$ - zone axes, respectively. All diffraction spots in these patterns can be fundamentally indexed by a simple cubic cell with lattice parameters of  $a = b = 0.383$  nm, in consistency with the reported data.<sup>2</sup> Due to the presence of structural domains, the weak diffuse streaking of the high-order reflection spots is also noted and will be analyzed in the following context.

A better and clear view of the atomic structural feature of the cubic crystal has been obtained by high-resolution TEM investigations. Fig. 2(c) and (d) show the high-resolution electron micrographs of  $\text{MgCNi}_3$  crystals taken along the  $\langle 001 \rangle$  and  $\langle 110 \rangle$  directions. These images were obtained from thin regions without clear structural inhomogeneity; therefore, we expect that, by comparing with the results of theoretical simulations, the Mg, C, and Ni atom positions could be identified. Image calculations were carried out by varying both the crystal thickness and the defocus value. A calculated  $[100]$  zone-axis image with the defocus value of 28 nm and the thickness of 3 nm is superimposed on the image of Fig. 2(c), and appears in good agreement with the experimental one. In this image the atom positions of Mg, Ni, and C/Ni are recognizable as bright dots with strong and weak intensities, respectively. We also include a corresponding calculated image on Fig. 2(d), which is obtained with the defocus value of 60 nm and the crystal thickness of 2.5 nm. In this experimental image Ni and Mg/Ni atom positions are recognizable as bright dots, and C atoms only yield weak gray contrast.

Now we go on to discuss the inhomogeneous properties appearing commonly in the superconducting materials with the nominal compositions of  $\text{Mg}_x\text{C}_y\text{Ni}_3$  ( $1.1 < x < 1.2, 1.2 < y < 1.50$ ). Basically, many materials exhibit complex domain. An example of this behavior is shown in the image of Fig. 3(a). This bright-field TEM image was obtained in a sample with nominal composition of  $\text{Mg}_{1.1}\text{C}_{1.2}\text{Ni}_3$ . Complex struc-

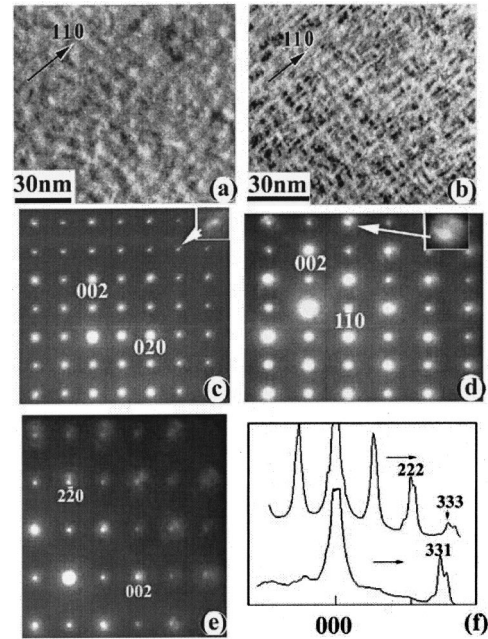


FIG. 3. (a) Complex structural domains in  $\text{Mg}_{1.1}\text{C}_{1.2}\text{Ni}_3$ ; (b) ordered domains in  $\text{Mg}_{1.2}\text{C}_{1.4}\text{Ni}_3$ , ordering behaviors occur along the  $\langle 110 \rangle$  and  $\langle 1-10 \rangle$  directions. Electron diffraction patterns along (c)  $\langle 001 \rangle$  and (d)  $\langle 110 \rangle$  directions, showing the splitting and streaking of the diffraction spots as clearly displayed in the insets. (e) A nanodiffraction pattern taken at an area with domains showing the presence of two-structure phases. (f) Microdensitometer traces showing the additional reflection peaks in  $\langle 111 \rangle$  and  $\langle 133 \rangle$  directions.

tural domains ranging from 5 to 20 nm can be clearly recognized. On the other hand, well-ordered domains have been frequently observed in the superconducting  $\text{Mg}_{1.2}\text{C}_{1.4}\text{Ni}_3$ . For instance, we display a bright-field TEM image in Fig. 3(b) taken along the  $\langle 001 \rangle$  direction. It clearly shows the structural domains with an average size as small as  $\sim 4$  nm along the  $\langle 110 \rangle$  and  $\langle 1-10 \rangle$  directions.

In order to understand the origin of this kind of domain structures, we have performed a systematical analysis based on electron diffraction, energy dispersive x ray (EDX) microanalysis, and high-resolution TEM observations. Fig. 3(c) and (d) show the SAED patterns taken at the areas with evident structural domains. The notable feature revealed in electron diffraction patterns is found to be the splitting and diffuse streaking of the diffraction spots, as clearly illustrated in the insets of the diffraction patterns. EDX analyses on the crystalline grains suggest that the superconducting phase have the composition of  $\text{MgC}_y\text{Ni}_3$  with  $y$  in a limited range of  $0.92 < y < 1$ , which could slightly vary with the nominal compositions of the samples. These results are in good agreement with that reported data in Ref. 2, where the superconducting phase is proposed to be  $\text{MgC}_{0.96}\text{Ni}_3$ . Excess carbon and Mg added to the initial mixtures are likely to be in connection with the appearance of some impurity phases, and remarkably, which also leads to drastic changes of microdomain structures in the resultant samples. Nanodiffraction ( $\sim 30$  nm in probe size) on areas with clear domains revealed evidently the coexistence of two kinds of structures in the

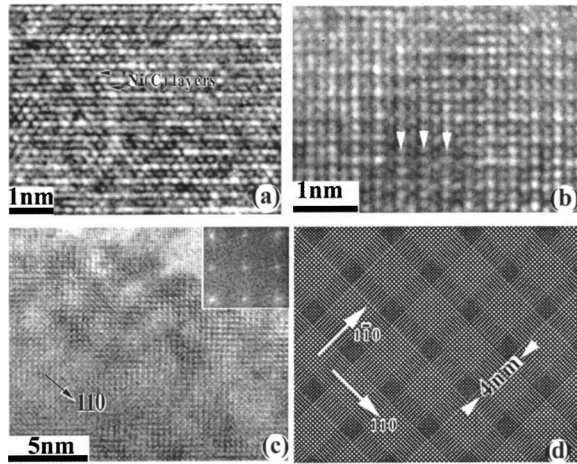


FIG. 4. (a) High-resolution TEM image taken slightly off the  $\langle 111 \rangle$  direction, exhibiting the strong dot contrast in the C/Ni layers. (b) The  $[001]$  TEM image taken at a thin area of the superconducting crystal, showing evident structural distortion. (c) TEM image of two-dimensional ordered domains in  $\text{Mg}_{1.2}\text{C}_{1.4}\text{Ni}_3$ , inset displays the Fourier transform showing split of reflection spots. (d) Schematic illustration of the regular domains arising from the coexistence of  $\text{MgCNi}_3$  and C-deficient phase  $\text{MgC}_{0.75}\text{Ni}_3$ .

superconducting samples, Fig. 3(e) show a nanodiffraction pattern taken by tilting slightly off the  $[110]$ -zone axis, clearly illustrating the presence of two sets of reflection spots. The systematic analysis indicated that the domains in superconducting phase originate from an additional local structural phase with different lattice parameters. In order to estimate the lattice parameters of this local phase, we have analyzed a set of diffraction patterns and obtained the microdensitometer traces along several relevant directions, two examples of these data are shown in Fig. 3(f), clearly displaying the additional reflection peaks. The local structural phase is determined to be a cubic structure with lattice parameters of  $3.7 \text{ \AA} < a < 3.8 \text{ \AA}$ . This parameter could change slowly from sample to sample. According to the previously reported data for the  $\text{MgC}_x\text{Ni}_3$  materials,<sup>5,7</sup> there are two notable structural phases: (a) the conventional phase  $\text{MgC}_x\text{Ni}_3$  ( $x \sim 1$ ), it has a cubic structure with lattice parameter  $a = 0.383 \text{ nm}$ .<sup>7</sup> This phase is believed to play an important role for the formation of superconductivity in the present system; (b) the C-deficient phase  $\text{MgC}_{0.75}\text{Ni}_3$ , which also has a cubic structure with lattice parameter  $a = 0.376 \text{ nm}$ .<sup>5</sup> This phase is likely to exist locally in the superconducting materials.

The microstructure and lattice distortion, associated with the structural domains, has been investigated by high-resolution TEM studies. Fig. 4(a) is a high-resolution TEM image taken slightly off the  $\langle 110 \rangle$  direction, the anomalous contrast in many areas can clearly recognized as singular dots, locating commonly within the C(Ni) layers. Fig. 4(b) shows the structural lamellae in the superconducting crystal. The local concentration of singular dots results in evident

contrast anomaly in association with structural variation. In the areas with uniform contrast two-dimensional lattice structure are well resolved, nevertheless, in the distorted areas one-dimensional lattice, as indicated by arrows, become clearly visible. This kind of structural alteration originates locally from a distinguished reduction of the lattice-cell volume of the C-deficient phase. e.g.,  $\text{MgC}_{0.75}\text{Ni}_3$  phase has a  $\sim 4.3\%$  contraction in volume. We have made numerous attempts to directly measure the modifications of crystal lattices from the high resolution TEM images, however, due to the presence of strain relaxation in the thin areas and local orientational alternation, it is difficult to get an accurate result. High-resolution TEM images frequently revealed the well-ordered domains in the superconducting sample of  $\text{Mg}_{1.2}\text{C}_{1.4}\text{Ni}_3$ . Fig. 4(c) shows the high-resolution TEM image of an area with clear ordered domains within the  $a$ - $b$  plane. Structural variations in association with regular alternation of contrast could appear in the  $\langle 110 \rangle$  direction and the other crystallographically related ones. This ordered structural feature can be roughly illustrated by a modulated structure with wave vector  $q = (\beta, \beta, 0)$  with  $\beta \sim 1/15$ . Fig. 4(d) displays a schematic illustration of this structural feature. An extensive investigation about the local structural distortion, C deficiency in this superconductor and their effects on superconductivity is in progress. Based on our structural investigations, we could make a brief estimation about the composition of the superconducting phase in the  $\text{Mg}_{1.2}\text{C}_{1.4}\text{Ni}_3$  material. In the high-resolution TEM images the average distance between the distorted segments is about 15 times (110) planar spacing of the lattice,  $d_{110} = 0.27 \text{ nm}$ . The occurrence ratio of the C-deficient phase, assumed to be  $\text{MgC}_{0.75}\text{Ni}_3$ , is around 15–25%, which could give rise to average composition of the superconducting phase ranging from  $\text{MgC}_{0.94}\text{Ni}_3$ – $\text{MgC}_{0.96}\text{Ni}_3$ , this result is consistent with our EDX data.

In conclusion, essential inhomogeneity appears commonly in the superconducting samples with nominal composition of  $\text{Mg}_x\text{C}_y\text{Ni}_3$  ( $1.1 < x < 1.2, 1.2 < y < 1.4$ ). Well-ordered domains exhibit in the sample with sharp superconducting transition at the temperature of 7 K. This structural feature has been qualitatively explained in terms of the perovskite cubic phase  $\text{MgCNi}_3$  modulated locally by the appearance of the second phase  $\text{MgC}_{0.75}\text{Ni}_3$  with smaller lattice parameters. The common appearance of inhomogeneity in present system is fundamentally connected with the variable stoichiometry on the C sites. In addition, this kind of defects could lead to the modification of the charge-carrier density in superconducting materials, and may play an important role for the understanding of the superconductivity in present system.

This work was supported by the U.S. Department of Energy, Division of Material Science, Office of Basic Energy Science, under Contract No. DE-AC02-98CH10886.



- <sup>1</sup>J. Nagamatsu, N. Nakagawa, T. Muranaka, Y. Zenitani, and J. Akimitsu, *Nature (London)* **410**, 63 (2001).
- <sup>2</sup>T. He, Q. Huang, A. P. Ramirez, Y. Wang, K. A. Regan, M. A. Hayward, M. K. Haas, J. S. Slusky, K. Inumaru, H. W. Zandbergen, N. P. Ong, and R. J. Cava, *Nature (London)* **411**, 54 (2001).
- <sup>3</sup>Z. Q. Mao, M. M. Rosario, K. Nelson, K. Wu, I. G. Deac, P. Schier, Y. Liu, T. He, K. A. Regan, and R. J. Cava, cond-mat/01053280 (unpublished).
- <sup>4</sup>E. Scheil and Z. Huetter, *Metallk* **44**, 387 (1953).
- <sup>5</sup>L. J. Huetter and H. H. Stadelmaier, *Acta Metall.* **6**, 367 (1958).
- <sup>6</sup>Z. A. Ren, G. C. Che, S. L. Jia, H. Chen, Y. M. Ni, and Z. X. Zhao, cond-mat/0105366 (unpublished).
- <sup>7</sup>B. Bogdanovic, K.-H. Claus, and U. Wilczok, *J. Less-Common Met.* **131**, 167 (1987).